



# The Threatening Magnetic and Plasma Environment of the TRAPPIST-1 Planets

Cecilia Garraffo<sup>1</sup>, Jeremy J. Drake<sup>1</sup>, Ofer Cohen<sup>1,2</sup>, Julian D. Alvarado-Gómez<sup>1</sup>, and Sofia P. Moschou<sup>1</sup>

<sup>1</sup>Harvard-Smithsonian Center for Astrophysics, 60 Garden Street, Cambridge, MA 02138, USA

<sup>2</sup>Lowell Center for Space Science and Technology, University of Massachusetts Lowell, 600 Suffolk Street, Lowell, MA 01854, USA

Received 2017 April 14; revised 2017 May 19; accepted 2017 June 13; published 2017 July 12

## Abstract

Recently, four additional Earth-mass planets were discovered orbiting the nearby ultracool M8 dwarf, TRAPPIST-1, making a remarkable total of seven planets with equilibrium temperatures compatible with the presence of liquid water on their surface. Temperate terrestrial planets around an M-dwarf orbit close to their parent star, rendering their atmospheres vulnerable to erosion by the stellar wind and energetic electromagnetic and particle radiation. Here, we use state-of-the-art 3D magnetohydrodynamic models to simulate the wind around TRAPPIST-1 and study the conditions at each planetary orbit. All planets experience a stellar wind pressure between  $10^3$  and  $10^5$  times the solar wind pressure on Earth. All orbits pass through wind pressure changes of an order of magnitude and most planets spend a large fraction of their orbital period in the sub-Alfvénic regime. For plausible planetary magnetic field strengths, all magnetospheres are greatly compressed and undergo much more dynamic change than that of the Earth. The planetary magnetic fields connect with the stellar radial field over much of the planetary surface, allowing the direct flow of stellar wind particles onto the planetary atmosphere. These conditions could result in strong atmospheric stripping and evaporation and should be taken into account for any realistic assessment of the evolution and habitability of the TRAPPIST-1 planets.

*Key words:* magnetohydrodynamics (MHD) – methods: numerical – planets and satellites: general – stars: activity – stars: individual (TRAPPIST-1) – stars: winds, outflows

## 1. Introduction

The recent discovery of four additional planets around TRAPPIST-1 with masses and radii similar to the Earth's (Gillon et al. 2017), combined with the three already known (Gillon et al. 2016), makes this system of special importance for characterizing terrestrial exoplanetary atmospheres and their evolution.

TRAPPIST-1 is an ultracool dwarf (M8V) 12 pc from the Sun with a mass of  $\sim 0.08 M_{\odot}$  and a radius of  $R_{\star} = 0.114 R_{\odot}$ . Its seven confirmed planets are in a coplanar system viewed nearly edge-on. All of the planets reside very close to the host star at distances from 0.01 to 0.063 au (for comparison, Mercury is at 0.39 au), with orbital periods from 1.5 to 20 days.

The atmospheres of close-in exoplanets are vulnerable to strong energetic (UV to X-ray) radiation and intense stellar wind conditions that could lead to atmospheric stripping (Lammer et al. 2003; Cohen et al. 2014, 2015; Garraffo et al. 2016). This is particularly important for planets in the habitable zones of M dwarfs whose low bolometric luminosities mean that temperate orbits lie very close to the parent star. Even a substantial underestimation of the actual XUV emission of TRAPPIST-1 suggests that planets b and c could have lost up to 15 Earth oceans, while up to one Earth ocean could have escaped from planet d (Bolmont et al. 2017; Wheatley et al. 2017). Climate models suggest that planet e represents the best chance for the presence of liquid water on its surface (Wolf 2017). In addition, the frequent flaring activity of TRAPPIST-1 is expected to make the conditions on its planets less favorable for hosting life (Vida et al. 2017). The capacity of these planets to have retained any water at all will depend critically on the initial water reservoir and on the erosive action of the stellar wind.

Stellar magnetic activity responsible for UV–X-ray emission and the generation of hot, magnetized winds in Sun-like stars is driven largely by stellar rotation. This influence extends from early F-spectral types down to M9 and stars in the fully convective regime (Wright et al. 2011; Wright & Drake 2016). Activity increases with the rotation rate up to a saturation limit beyond which faster rotation no longer results in further increase. Activity also appears to decline in very low-mass stars and brown dwarfs with spectral types later than M9 (Berger et al. 2010).  $H_{\alpha}$  observations of TRAPPIST-1 (Reiners & Basri 2010) put its magnetic activity as high as the saturation regime, consistent with its M8 spectral type and short rotation period of  $P_{\text{rot}} = 3.3$  days (Luger et al. 2017, recently revised from 1.4 days; Gillon et al. 2017). X-ray observations (Cook et al. 2014; Wheatley et al. 2017) confirm it has a hot corona with a ratio of X-ray to bolometric luminosity,  $L_X/L_{\text{bol}} = (2-4) \times 10^{-4}$ , within the observed scatter around the saturation limit of  $L_X/L_{\text{bol}} \sim \times 10^{-3}$  (Wright et al. 2011). TRAPPIST-1 is then fully expected to have a solar-like wind consistent with that of the observed spin-down of fully convective M dwarfs (e.g., Irwin et al. 2011), which could be a destructive agent of planetary atmospheric loss.

In earlier work, we used a state-of-the-art magnetohydrodynamic (MHD) code to model the stellar winds and magnetospheres of systems around M dwarfs and studied the space environment and atmospheric impact for planets in the “habitable zone” (Cohen et al. 2014, 2015; Garraffo et al. 2016). With its planets even closer in to the star than that of the case of Proxima and Proxima b considered by Garraffo et al. (2016), the TRAPPIST-1 system is sufficiently different to warrant further study. Here, we use a similar technique to model the space weather conditions of the planets around TRAPPIST-1 and make the further important step of computing the response of the planetary magnetospheric structure to the stellar wind.



Original content from this work may be used under the terms of the [Creative Commons Attribution 3.0 licence](https://creativecommons.org/licenses/by/3.0/). Any further distribution of this work must maintain attribution to the author(s) and the title of the work, journal citation and DOI.

## 2. Magnetohydrodynamic Modeling

### 2.1. Method

We use the *BATS-R-US* MHD code (van der Holst et al. 2014) to model the TRAPPIST-1 stellar system. The simulation results are obtained using the Alfvén Wave Solar Model (AWSoM; van der Holst et al. 2014), which is the Solar Corona module of the *BATS-R-US* MHD code. The model is driven by the photospheric stellar magnetic field data and it solves the set of non-ideal MHD equations on a spherical grid.

The MHD equations include the conservation of mass, momentum, and magnetic flux and energy. In order to provide a hot corona and stellar wind acceleration, two additional equations are solved for the counter-propagating Alfvén waves along the two opposite directions of magnetic field lines, where the model accounts for the dissipation of energy as a result of a turbulent cascade. The two equations for the two Alfvén waves are coupled to the energy equation via a source term, and to the momentum equation via an additional wave pressure term.

In the energy equation, the code also accounts for thermodynamic effects, such as radiative cooling and electron heat conduction. Due to the lack of information about the level of MHD turbulence in other stars such as M dwarfs with strong magnetic fields, the model embeds a scaling relation between the stellar field and the total heating via the relation between the observed total magnetic flux and X-ray flux from solar features and stars (Pevtsov et al. 2003). Thus, the parameter that controls the amount of heat flux,  $L_{\text{perp}}$  in van der Holst et al. (2014), scales with the square root of the average magnetic field on the stellar surface. We scale this parameter for the M-dwarf star with respect to the validated value for the solar case. For full details of the model and the references for the theoretical models which are implemented, we refer the reader to van der Holst et al. (2014).

The model uses a map of the 2D surface distribution of the stellar radial magnetic field (a “magnetogram”) as the inner boundary condition. For stars, these magnetograms are typically obtained using high-resolution spectropolarimetry and the Zeeman–Doppler Imaging (ZDI) technique (Semel 1980; Donati & Brown 1997). The initial condition for the 3D magnetic field is obtained by calculating the analytical solution to Laplace’s equation assuming that the field is potential, i.e., a static magnetic field with no currents forcing its change. Once the MHD solution starts to evolve, the currents represented by the evolving stellar wind begin to affect the initial, static magnetic field until a steady state is achieved. By including all the terms above, the stellar input parameters for the mass, radius, and rotation period, as well as the photospheric field data, the model provides a self-consistent, steady-state solution for the hot corona and stellar wind from the stellar chromosphere out to the extent of the adopted model grid. The models presented here employed adaptive mesh refinement with a maximum resolution of  $0.05 R_*$ .

Evans et al. (2008) compared different models for coronal heating and wind acceleration including empirical, semi-empirical, and Alfvén wave heating. They concluded that the only type of models that provide good agreement with coronal signatures are those with Alfvén wave heating, as employed by the AWSoM model. This numerical approach is currently used for the space weather forecast in the solar system, and has been validated against observations in several works (e.g., Meng et al. 2015; Alvarado-Gómez et al. 2016a, 2016b).

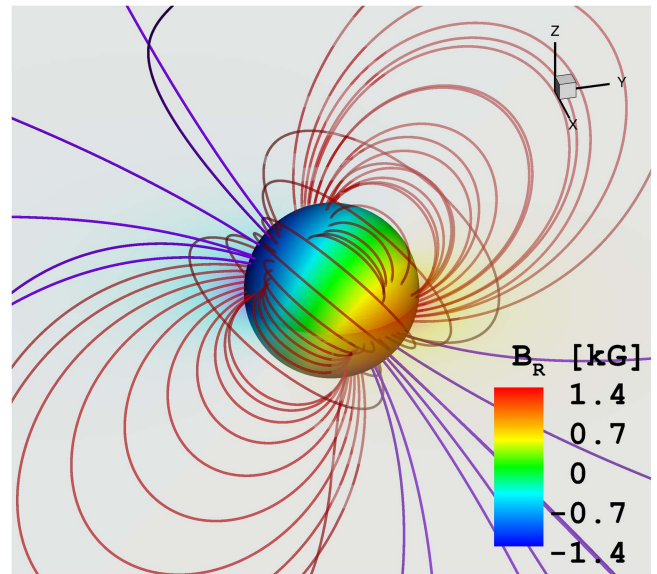


**Figure 1.** Magnetogram for GJ 3622 with 600 G average field strength. Closed field lines are colored in red and open field lines are colored in purple.

Furthermore, AWSoM has been tested and validated by extreme ultraviolet observations of Sun and its immediate vicinity (van der Holst et al. 2014), which is the regime we wish to explore in this work for the close-in planets in TRAPPIST-1.

In order to study the interaction between the extreme stellar wind and the upper atmosphere of one of the TRAPPIST-1 planets, we use the Global Magnetosphere module of *BATS-R-US*. This module is driven by the upstream stellar wind conditions as extracted from the AWSoM model.

### 2.2. Calculations

Unfortunately, TRAPPIST-1 is too faint ( $M_V = 18.4$ ) to obtain ZDI maps with current instrumentation. However, the average magnetic field strength was measured using Zeeman Broadening to be 600 G (Reiners & Basri 2010). Empirically, the distribution of surface magnetic field at a given spectral type is found to depend mainly on the rotation rate (Vidotto et al. 2014; Garraffo et al. 2015; Réville et al. 2015). To model the system we can then use as a proxy the ZDI magnetogram of a star with parameters most similar to those of TRAPPIST-1 available. We adopt the magnetogram of GJ 3622 (Morin et al. 2010), an M6.5 dwarf with a rotation period of 1.5 days, shown in Figure 1. In addition, we have performed simulations for the recently revised rotation period of 3.3 days (Luger et al. 2017) and find that the results are unaltered. This is expected since the magnetic field strength estimation is unchanged and other effects of fast rotation, like magnetic field wrapping, only become important at shorter rotation periods of less than a day. We use the observed relative orientation of the magnetic fields with respect to the rotation axis. The range of mean surface field strengths allowed by the Reiners & Basri (2010) measurement is about 200–800 G. In order to understand the influence of the mean surface magnetic field strength on the results, we probe two magnetic field scalings of the magnetogram, one to match the  $\sim 600$  G surface field measurement, and one with half of that value.

As a test, we also computed models for the magnetogram of the very late dwarf, VB 10 (Morin et al. 2010), using the

TRAPPIST-1 rotation period. While VB 10 has the same M8 spectral type as TRAPPIST-1, its own rotation period is currently uncertain, with values of 0.52 and 0.69 days favored. The magnetogram was reconstructed for the latter but is consequently subject to considerable uncertainty. We found wind conditions at the TRAPPIST-1 planetary orbits to be quite similar to those of our GJ 3622 proxy model. The reason is that the dominant factors responsible for the extreme space weather environment in these kind of systems are the high plasma densities and pressures that the close-in planets reside in, which in turn depend on the stellar magnetic field strength. For VB 10, this is similar to that of our proxy. We do not discuss the VB 10 results further, and instead concentrate on our TRAPPIST-1 proxy simulations.

The MHD model of the stellar corona, wind, and magnetic field of TRAPPIST-1 was driven using its measured mass, radius, and rotation period,  $M = 0.08 M_{\odot}$ ,  $R = 0.114 R_{\odot}$ , and  $P_{\text{rot}} = 1.4$  days, respectively. From the resulting 3D wind structure, illustrated in Figure 2, we extracted the wind pressure values over all the planetary orbits. The semimajor axes are known and range from 0.011 to 0.063 au, all the eccentricities are constrained to be smaller than 0.085, and the inclinations of the orbits with respect to the observer’s line of sight are nearly  $90^{\circ}$ . We assume that this very nearly coplanar system of planets has an orbital axis aligned with the star’s rotation axis. Therefore, we model the seven circular orbits with their observed planetary parameters on the equatorial plane.

All the planets detected around TRAPPIST-1 have Earth-like masses, and we examine planetary magnetic fields with equatorial strengths of 0.1 and 0.5 G that bracket the present day terrestrial value of 0.3 G.

We are confident that we have produced the most realistic wind model one can currently make for TRAPPIST-1. Mass loss and angular momentum loss rates can be used to calculate spin-down timescales. We find mass loss rates of  $\sim 3 \times 10^{-14} M_{\odot} \text{ yr}^{-1}$  and angular momentum loss rates of  $\sim 6 \times 10^{30}$  erg, which are expected for a rapidly rotating M dwarf and consistent with the currently quite uncertain picture of their rotational evolution timescales (see, e.g., Basri & Marcy 1995; West et al. 2008; Irwin et al. 2011).

To assess the magnetospheric response of the TRAPPIST-1 planets to the stellar wind using the Global Magnetosphere module, we examine the case of Trappist-1 f. This is the central planet of the three potentially habitable planets (e, f, and g). We extract the wind conditions at one sub-Alfvénic point and one super-Alfvénic point along the orbit. Once the upstream conditions are set at the outer boundary of the simulation domain, a steady-state solution for the magnetosphere is obtained. The inner boundary is set at  $r = 2 R_{\oplus}$ , and the boundary conditions we assume here are the same as those used in Earth magnetosphere simulations. A model for the Ionospheric Electrodynamics is also used to better set the velocity at the boundary as described in Cohen et al. (2014).

### 3. Results and Discussion

Figure 2 illustrates the 3D wind speed and density for TRAPPIST-1 from our simulations, corresponding to the 600 G observed average magnetic field strength. The seven known planetary orbits are plotted together with the 3D Alfvén surface. Wind speeds reach close to  $1400 \text{ km s}^{-1}$  and are only slightly higher than the  $800\text{--}900 \text{ km s}^{-1}$  typical of the fast

solar wind (McComas et al. 2007). In contrast, the densities of the plasma that these planets go through reach  $10^4\text{--}10^5$  times the solar wind density at 1 au. In addition, the planets lie much closer to the Alfvén surface than in the solar system. The solar wind Alfvénic critical point generally lies between 6 and  $20 R_{\odot} \approx 0.03\text{--}0.1$  au (DeForest et al. 2014)—well within the orbit of Mercury. Instead, all but the outermost TRAPPIST-1 planets spend a large fraction of their orbits in the sub-Alfvénic regime, crossing the Alfvén surface four times over their short orbital periods ( $<13$  days).

In Figure 3 we show the total ambient pressures (magnetic plus dynamic, neglecting thermal and orbital terms that are at least an order of magnitude smaller),  $P_{\text{tot}} = B^2/(4\pi) + \rho U^2$ , where  $B$  is the magnetic field strength,  $\rho$  is the plasma mass density, and  $U$  is the wind speed, normalized to that of the solar wind at Earth for each magnetic field scaling. We also show the Alfvén surface intersection with the orbital plane and the seven detected orbits. The total pressure at these close-in orbits ranges from 3 to 6 orders of magnitude higher than that of the solar wind pressure at 1 au. In addition, even in the presence of wind speeds comparable to the solar wind one, due to the extremely high densities of the plasma around these close-in planets shown in Figure 2, the ambient dynamic wind pressure they are exposed to is 3–4 orders of magnitude larger than the solar wind pressure at Earth.

Both the total and dynamic pressure over the seven orbits for each of the two explored magnetic field scalings are illustrated in more detail in the top panel of Figure 4. For the closer-in planets, the magnetic pressure dominates over the dynamic pressure, while the converse tends to be true for the very outer planets. In addition to the extreme pressure, we see that most orbits go through magnetic and dynamic pressure variations of up to an order of magnitude crossing the current sheet in the vicinity of the magnetic equatorial plane. For planet b, with an orbital period of only 1.51 days (Gillon et al. 2017), this happens on a timescale of only 3–4 hr. The most stable total pressure is along the orbits of planet d for the 600 G stellar field and planet c for the 300 G field, for which the large increase in dynamic pressure when crossing the current sheet compensates for the dip in magnetic pressure.

One diagnostic of the effect of wind conditions on a magnetized planet is the magnetopause location, whose standoff distance from the planet can be approximated by assuming pressure balance between the planetary magnetic pressure and the wind total pressure (e.g., Schield 1969; Gombosi 2004),

$$R_{\text{mp}}/R_{\text{planet}} = [B_p^2/(4\pi P_{\text{tot}})]^{1/6},$$

where  $R_{\text{mp}}$  is the radius of the magnetopause,  $R_{\text{planet}}$  is the radius of the planet,  $B_p$  refers to the planetary equatorial magnetic field strength, and  $P_{\text{tot}}$  is the ram pressure of the stellar wind combined with that of the stellar magnetic field pressure. The magnetopause distance as a function of orbital phase for the seven different orbits considered and for the two stellar magnetic field scalings is illustrated in Figure 4 (bottom panel). If these planets have magnetospheres, they would be much smaller than that of the Earth, which has a standoff distance of  $\sim 10 R_{\oplus}$  (Pulkkinen 2007). However, according to our simulations, most of the TRAPPIST-1 planets reside in the sub-Alfvénic regime for large fractions of their orbital period.

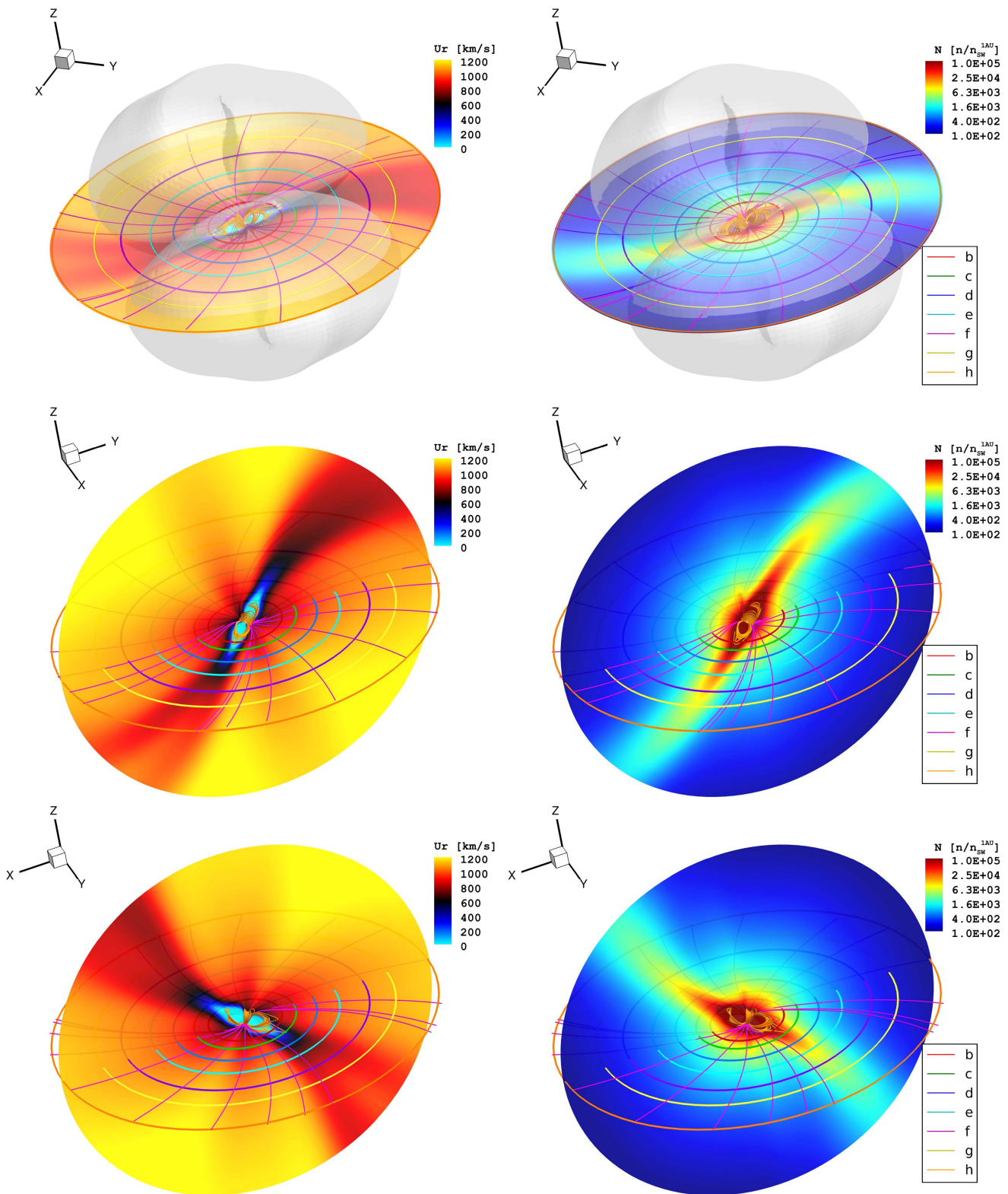
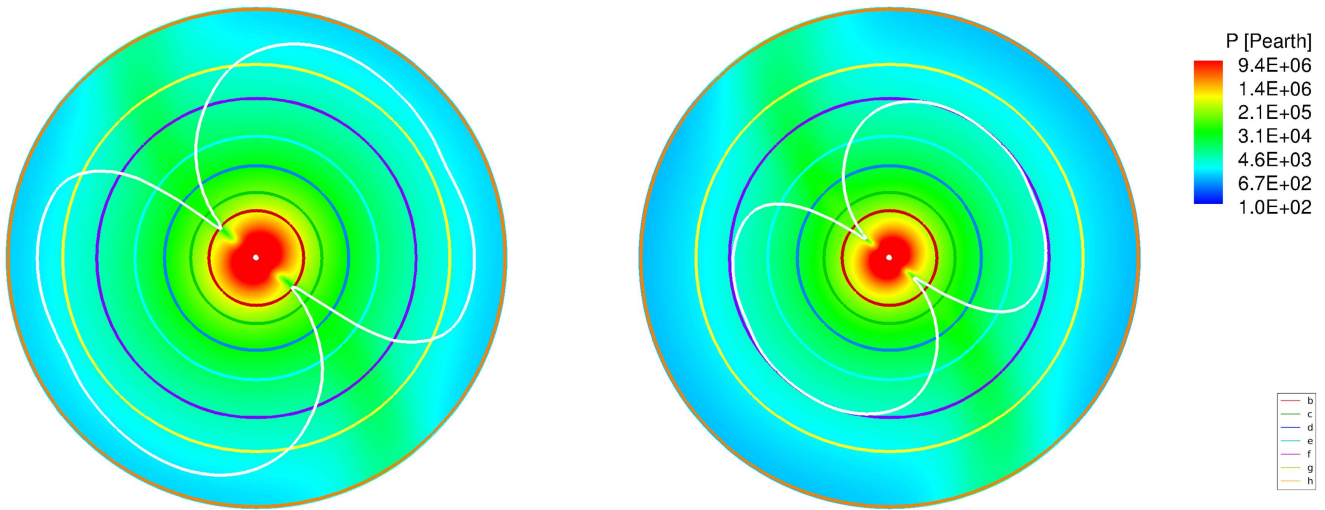


**Figure 2.** Three-dimensional stellar magnetosphere and wind for TRAPPIST-1 simulated using a magnetogram for the proxy star GJ 3622 with an average field strength of 600 G. The orbital plane (top row) and two meridional cuts ( $x = 0$ , middle;  $y = 0$ , bottom two rows) are presented. The color bar denotes the wind speed (left), and density normalized to solar wind values at 1 au (right). The gray shaded surface in the top panels corresponds to the Alfvén surface. Selected closed (orange) and open (purple) magnetic field lines are shown. All of the known orbits are plotted.

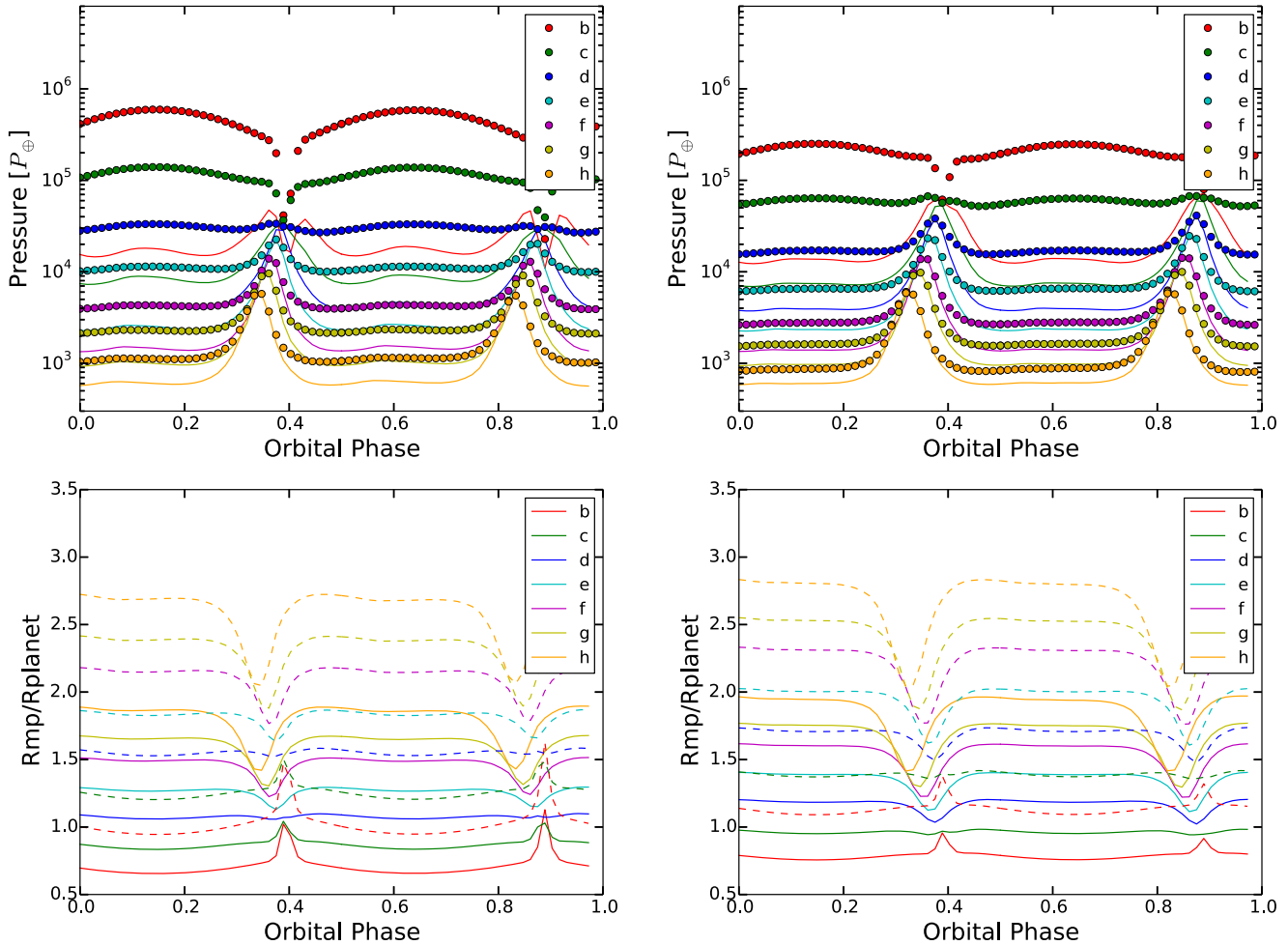
For this reason, we go a step further and simulate directly the wind-exoplanet interaction using a global magnetosphere model.

Figure 5 shows the magnetospheric structure of TRAPPIST-1 f as calculated using the Global Magnetosphere module of

*BATS-R-US*. Trappist-1 f provides a representative case of the three potentially habitable planets e, f, and g, and from Figure 4 it can be seen that the stellar wind conditions around the three are quite similar. Here, we make a specific assumption that the



**Figure 3.** Total ambient pressure normalized to the solar wind pressure at 1 au for all the detected orbits of TRAPPIST-1 for a mean stellar magnetic field of 600 G (left) and 300 G (right). The Alfvén surface is shown in white.



**Figure 4.** Top panel: total pressure (filled circles) and dynamic pressure (lines) normalized to the solar wind at 1 au for all the planetary orbits assuming the measured stellar magnetic field strength of  $\sim 600$  G (left) and half of that ( $\sim 300$  G, right). Bottom panel: magnetosphere standoff distance normalized to the planet’s radius for all the planetary orbits for the same  $\sim 600$  G (left) and  $\sim 300$  G (right) stellar magnetic fields. Dashed and solid lines correspond to a 0.5 G and 0.1 G planetary magnetic field, respectively.

planet is magnetized and the planetary field is similar to that of the Earth as there is no available data to constrain the planetary field.

Planet f resides in a region that is dominated by strong radial components of both the stellar wind velocity and magnetic

field. The extreme wind pressure (dynamic and magnetic in the case of the sub-Alfvénic regions) opens the planetary field all the way to the planetary surface, creating what is essentially a very large polar cup (open field region) that extends over most

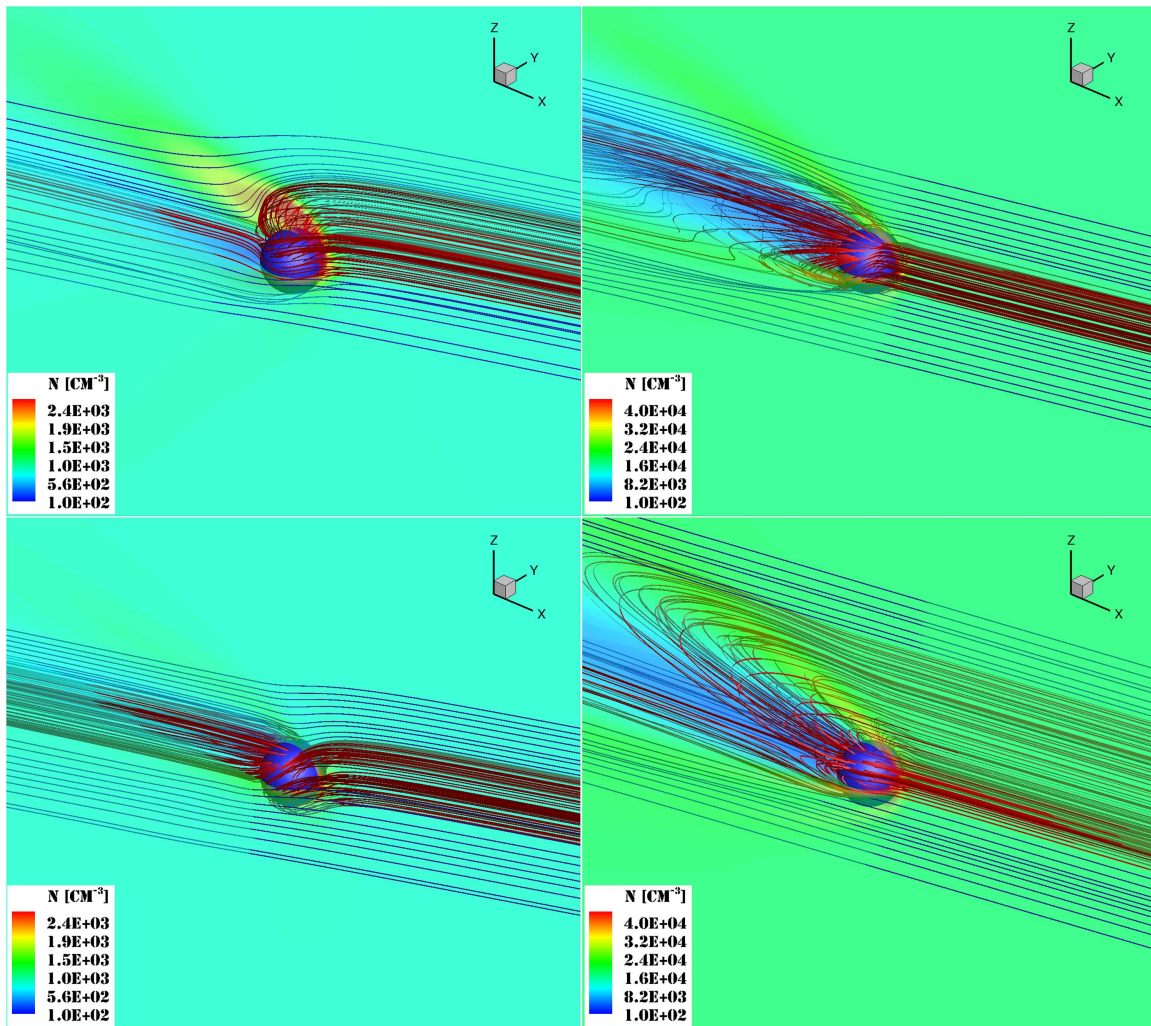


**Figure 5.** Magnetospheric structure of TRAPPIST-1 f assuming a planetary magnetic field the same as the that of the Earth (top panels), and an Earth field with an opposite sign (bottom panels). The star is located on the right along the  $x$ -axis and the sphere represents the planet. The solutions are for sub-Alfvénic (left panels) and super-Alfvénic (right panels) stellar wind conditions as extracted from the stellar wind model. Field lines that are connected to the planet are shown in red, while nearby stellar field lines are shown in blue. These results are for a stellar field of 600 G. The magnetospheric solutions for the 300 G field were very similar.

of the planet. This is a new regime not experienced in solar system planets; there is no magnetopause at which the planetary field pressure balances the wind pressure. Instead, stellar wind particles can constantly precipitate directly down open field onto the atmosphere. The concept of atmospheric protection by a planetary magnetic field does not hold here and is likely not to hold in the conventional sense for the TRAPPIST-1 planets. The TRAPPIST-1 system represents a new challenge to atmospheric evolution and survival on close-in planets around very low-mass stars.

C.G. thanks Rakesh K. Yadav for the useful comments and discussions. C.G. was supported by SI Grand Challenges grant “Lessons from Mars: Are Habitable Atmospheres on Planets around M Dwarfs Viable?” J.J.D. was supported by NASA contract NAS8-03060 to the *Chandra X-ray Center*. O.C. and S.P.M. are supported by NASA Astrobiology Institute grant NNX15AE05G. J.D.A.G. was supported by *Chandra* grants AR4-15000X and GO5-16021X. This work was carried out using the SWMF/BATSRUS tools developed at The University of Michigan Center for Space Environment Modeling (CSEM) and made available through the NASA Community

Coordinated Modeling Center (CCMC). Simulations were performed on NASA’s PLEIADES cluster under award SMD-16-6857.

## References

- Alvarado-Gómez, J. D., Hussain, G. A. J., Cohen, O., et al. 2016a, *A&A*, **588**, A28  
 Alvarado-Gómez, J. D., Hussain, G. A. J., Cohen, O., et al. 2016b, *A&A*, **594**, A95  
 Basri, G., & Marcy, G. W. 1995, *AJ*, **109**, 762  
 Berger, E., Basri, G., Fleming, T. A., et al. 2010, *ApJ*, **709**, 332  
 Bolmont, E., Selsis, F., Owen, J. E., et al. 2017, *MNRAS*, **464**, 3728  
 Cohen, O., Drake, J. J., Gloer, A., et al. 2014, *ApJ*, **790**, 57  
 Cohen, O., Ma, Y., Drake, J. J., et al. 2015, *ApJ*, **806**, 41  
 Cook, B. A., Williams, P. K. G., & Berger, E. 2014, *ApJ*, **785**, 10  
 DeForest, C. E., Howard, T. A., & McComas, D. J. 2014, *ApJ*, **787**, 124  
 Donati, J.-F., & Brown, S. F. 1997, *A&A*, **326**, 1135  
 Evans, R. M., Opher, M., Manchester, W. B., IV, & Gombosi, T. I. 2008, *ApJ*, **687**, 1355  
 Garraffo, C., Drake, J. J., & Cohen, O. 2015, *ApJ*, **813**, 40  
 Garraffo, C., Drake, J. J., & Cohen, O. 2016, *ApJL*, **833**, L4  
 Gillon, M., Jehin, E., Lederer, S. M., et al. 2016, *Natur*, **533**, 221  
 Gillon, M., Triaud, A. H. M. J., Demory, B.-O., et al. 2017, *Natur*, **542**, 456  
 Gombosi, T. I. 2004, in *Physics of the Space Environment* (Cambridge: Cambridge Univ. Press), 357

- Irwin, J., Berta, Z. K., Burke, C. J., et al. 2011, *ApJ*, 727, 56
- Lammer, H., Selsis, F., Ribas, I., et al. 2003, *ApJL*, 598, L121
- Luger, R., Sestovic, M., Kruse, E., et al. 2017, arXiv:1703.04166
- McComas, D. J., Velli, M., Lewis, W. S., et al. 2007, *RvGeo*, 45, 1004
- Meng, X., van der Holst, B., Tóth, G., & Gombosi, T. I. 2015, *MNRAS*, 454, 3697
- Morin, J., Donati, J.-F., Petit, P., et al. 2010, *MNRAS*, 407, 2269
- Pevtsov, A. A., Fisher, G. H., Acton, L. W., et al. 2003, *ApJ*, 598, 1387
- Pulkkinen, T. 2007, *LRSP*, 4, 1
- Reiners, A., & Basri, G. 2010, *ApJ*, 710, 924
- Réville, V., Brun, A. S., Matt, S. P., Strugarek, A., & Pinto, R. F. 2015, *ApJ*, 798, 116
- Schild, M. A. 1969, *JGR*, 74, 1275
- Semel, M. 1980, *A&A*, 91, 369
- van der Holst, B., Sokolov, I. V., Meng, X., et al. 2014, *ApJ*, 782, 81
- Vida, K., Kővári, Z., Pál, A., Oláh, K., & Kriskovics, L. 2017, *ApJ*, 841, 124
- Vidotto, A. A., Jardine, M., Morin, J., et al. 2014, *MNRAS*, 438, 1162
- West, A. A., Hawley, S. L., Bochanski, J. J., et al. 2008, *AJ*, 135, 785
- Wheatley, P. J., Louden, T., Bourrier, V., Ehrenreich, D., & Gillon, M. 2017, *MNRAS*, 465, L74
- Wolf, E. T. 2017, *ApJL*, 839, L1
- Wright, N. J., & Drake, J. J. 2016, *Natur*, 535, 526
- Wright, N. J., Drake, J. J., Mamajek, E. E., & Henry, G. W. 2011, *ApJ*, 743, 48